Preclinical evaluation of a pediatric airway stent for tracheobronchomalacia

Check for updates

Abhijit Mondal, PhD,[a] Junhyoung Ha, PhD,[b] Vickie Y. Jo, MD,[c] Fei-Yi Wu, MD,[d] Aditya K. Kaza, MD,[a] and Pierre E. Dupont, PhD[a]

ABSTRACT

Objectives: We sought to demonstrate in an animal model that helical stents made from a nickel titanium alloy called nitinol (NiTi) and designed for malacic airways could be delivered and removed without significant trauma while minimally impeding mucus clearance during the period of implantation.

Methods: Stents were delivered and removed from the tracheas of healthy 20 kg swine (n = 5) using tools designed to minimize trauma. In 4-week experiments, the stents were implanted on day 0, removed after 3 weeks, and swine were put to death after 4 weeks. Weekly bronchoscopies, radiographs, and mucus clearance examinations were performed in vivo. Hematoxylin and eosin staining and scanning electron microscopy imaging were used to evaluate foreign body response, tracheal tissue reaction, and damage and to measure unciliated regions.

Results: In all in vivo experiments, the stent was implanted and removed atraumatically. Mucus clearance was maintained throughout the experiment period. Hematoxylin and eosin-stained slides showed that foreign body response and tracheal tissue damage were localized to the stented subsections. Tracheal tissue reaction and damage was further restricted to the epithelium and submucosal layers. Scanning electron microscopy imaging revealed that the cilia were absent only over the contact area between the trachea and the wire forming the helical stent.

Conclusions: Helical nitinol stents designed to provide radial support for malacic airways were well tolerated in a porcine model, providing for mucus clearance while also enabling atraumatic removal. (J Thorac Cardiovasc Surg 2021;161:e51-60)

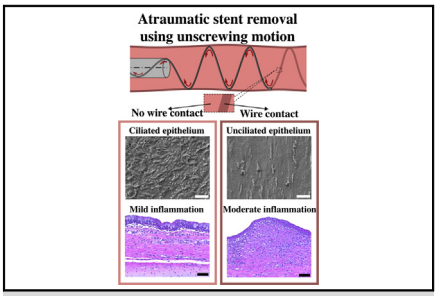

Helical stents limit inflammation and cilia damage where the stent wire contacts tissue.

CENTRAL MESSAGE

Preclinical testing of a new airway stent system that minimizes foreign body reaction, promotes mucus flow, and enables atraumatic removal.

PERSPECTIVE

We address the need for a pediatric airway stent that can provide an effective alternative to extended positive airway pressure ventilation as a treatment for tracheobronchomalacia. The proposed stent technology is demonstrated in short-term preclinical testing to circumvent the limitations of existing airway stents.

See Commentaries on pages e61 and e62.

Video clip is available online.

Tracheobronchomalacia is a rare disease in which a weakened or compressed airway impedes a child's respiration. For these children, during various phases of the respiratory cycle, the pleural pressure exceeds the intraluminal pressure resulting in airway collapse. Although a rare disease, it is the most common congenital defect of the central airway[1] with an incidence of at least 1 in 2100 children.[2] This condition affects not only respiration, but also a child's growth and development. Primary tracheobronchomalacia is typically caused by immature or malformed airway cartilage,

From the [a]Department of Cardiovascular Surgery, Boston Children's Hospital, Boston, Mass; [b]Center of Medical Robotics, Korea Institute of Science and Technology, Seoul, South Korea; [c]Department of Pathology, Brigham and Women's Hospital, Boston, Mass; and [d]Department of Surgery, Taipei Veteran General Hospital, Taipei City, Taiwan, Republic of China.

Supported by National Institutes of Health grant No. R21 HD089136 and R01 HL135077.

Received for publication Dec 10, 2019; revisions received March 2, 2020; accepted for publication March 3, 2020; available ahead of print March 15, 2020.

Address for reprints: Abhijit Mondal, PhD, Department of Cardiovascular Surgery, Boston Children's Hospital, 330 Longwood Ave, Enders Building 354, Boston, MA 02115 (E-mail: abhijit.mondal@childrens.harvard.edu).

0022-5223/$36.00

Copyright © 2020 by The American Association for Thoracic Surgery

https://doi.org/10.1016/j.jtcvs.2020.03.007

Abbreviations and Acronyms
CL = control
EtOH = ethyl alcohol
NiTi = nitinol
SEM = scanning electron microscopy
SNC = stented region with no wire contact
SWC = stented region with wire contact
UT = unstented

whereas secondary tracheobronchomalacia is associated with cartilage damage caused by prolonged intubation, surgery, or infection.[3,4] The standard treatment is positive pressure ventilation of 10 cm water or more, which raises the intraluminal pressure sufficiently to prevent collapse.[5-7] Extended ventilation is costly, and can involve chronic use of an endotracheal tube and carries the risk of airway infection.[5]

In adults, airway stents have been developed that are composed of solid silicone tubes.[8-10] These stents tend to migrate inside the airways and, furthermore, they completely obstruct the transitional epithelium lining of the trachea, which plays an important role in mucous secretion and mobilization of particulate debris. This creates a barrier that blocks mucociliary transport along the length of the stent. The relative thickness of the stent exacerbates the problem by reducing airway diameter resulting in inspissated secretions and frequent mucous plugging of the airways.[11] Mucus clearing is performed either by blind suctioning,[12,13] which risks stent migration, or by suctioning via bronchoscope. Consequently, even if sized for neonates and infants, such devices would be suboptimal and require close monitoring.

To find an alternative for neonates, some investigators have employed vascular metal mesh stents because they are available in smaller sizes.[14] The outcomes have matched those in adults; however, tissue growing through and covering the mesh makes stent removal difficult. Such concerns in adults led the Food and Drug Administration in 2005 to publish an advisory on the use of metallic tracheal stents in patients with benign airway disease.[15]

To avoid the need for stent removal, resorbable airway stents are being developed.[16-24] Resorbable designs tend to fragment during resorption and these fragments can migrate to and block the distal airways. Although the goal is to avoid reinterventions, weekly bronchoscopies are recommended to monitor the stent.[25-27] Furthermore, resorbing stents need to be replaced in those patients whose airways require extended support. It is unclear if the placement of a new stent over a previously implanted resorbing stent will exacerbate the fragmentation problem.

External resorbable splints have also been tested recently under the Food and Drug Administration's medical device emergency use exemption.[22] Although placement external to the trachea avoids the problem of loose fragments in the airway, the approach requires complex surgery involving extensive mobilization of the mediastinal structures. Consequently, if an effective stent was available, external splints would likely be reserved for patients who require surgery of the aortic arch or pulmonary arteries. Hence, there is a significant clinical need for a new approach that avoids the risks and costs of positive pressure ventilation and that does not share the major challenges of existing stents.

We investigated the feasibility of a stent and delivery/removal tool technology first proposed in our previous work.[28] The stents are helical coils of a nickel titanium alloy called nitinol (NiTi). While previous studies have reported helically shaped stents,[29-31] there are several distinguishing features of the stents described here. First, the stent geometry is optimized to introduce the minimum amount of foreign material into the airway while providing radial support equivalent to that of positive airway pressure; that is, 10 cm water. In particular, this involves solving for the maximum helical pitch and minimum wire diameter that produces the desired radial support.[28] This results in a stent design that minimizes foreign body reaction and does not impede mucus flow. Furthermore, we introduce a stent removal tool that enables the stent to be retracted into a cannula using an unscrewing motion that matches its helical pitch. If it is embedded in the epithelium, its removal is similar to a corkscrew being removed from a cork—there is minimal damage to the tissue. In our previous work[28] we described how to design the stent to provide sufficient airway support; this article provides a detailed assessment of stent performance through in vivo animal experiments.

MATERIALS AND METHODS

Stent and Tool Design and Function

The self-expanding helical stents, shown in Figure 1, *A*, are fabricated from superelastic NiTi wire with a ball of NiTi at each tip. The wire diameter and pitch of the helix can be designed as described elsewhere[28] to provide support comparable to a desired level of positive airway pressure (10 cm water). For this study, the wire diameter was 0.51 mm and the pitch was 18.6 mm. For delivery, the stent is compressed inside a delivery cannula (Figure 1, *B*) with its distance ball tip locked into an inner delivery cannula. Under bronchoscopic guidance (Karl Storz 10328AA, Tuttlingen, Germany), the delivery tool can be navigated to the desired location in the trachea or bronchi. The outer cannula (outer diameter, 6.5 mm) is slowly retracted to release the stent. The distal end of the stent is then released and the tool retracted.

The stent removal system is comprised of an outer cannula (outer diameter, 8 mm) connected to an inner pair of cup-shaped forceps by a screw connection matching the pitch of the helical stent (Figure 1, *C*). The forceps are initially extended from the cannula and, under endoscopic guidance, are used to grasp the ball on the proximal end of the stent, which may be partially or fully embedded in the epithelium. Once the stent's ball tip is grasped, the forceps are retracted by rotation with respect to the outer cannula. This screw motion causes the stent wire to retract in a follow-the-leader fashion into the cannula. Once the entire stent is inside the outer cannula, the tool is removed.

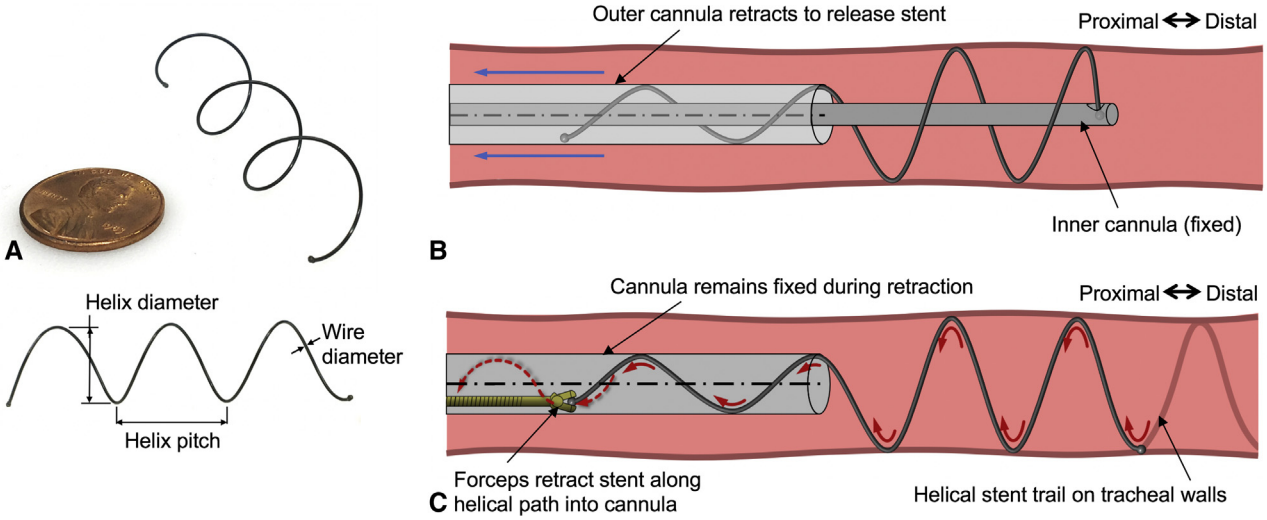

FIGURE 1. Helical nitinol (NiTi) stent system. A, Stent fabricated from 0.51 mm NiTi wire with stent design parameters labeled. Helix pitch and wire diameter were selected such that, under the expected pressure, the stent would not compress significantly while also preventing tissue between coils to collapse. B, Schematic showing the delivery of the stent at a desired location in the trachea. The stent is compressed inside the outer cannula with its distal end locked into a central canula and navigated to the desired stenting location in the trachea. Here, the stent is slowly released by retracting the outer canula while maintaining the position of the inner cannula. Once the stent is completely released from the outer canula, its distal end is released from the inner cannula. C, Schematic of atraumatic removal technique. The stent is removed like a screw (*red arrows*) leaving a helical trail on the trachea walls. This is accomplished by retracting the forceps grasping the stent in a helical path (*dotted red arrows*).

In Vivo Experiments

Survival experiments in Yorkshire swine were approved by the Institutional Animal Care and Use Committee of Boston Children's Hospital.

Animals (20 kg and aged 2 months) were acquired from a local breeder (Parsons Farm, Westhampton, Mass). Five experimental animals were used that received stents as described below. Two additional animals that did not undergo any tracheal procedures were also used as controls. Four-week experiments were performed with the stent placed on day 0 and removed on day 21. Bronchoscopy and radiographic imaging were performed every week. For the weekly procedures, the animal was induced with a regimen of telazol 4.5 mg/kg, xylazine 2 mg/kg, and atropine 0.04 mg/kg. The animal was maintained with intravenous propofol 3 to 5 mg/kg/hour.

For stent placement, tracheal diameter and length were estimated from a left lateral thoracic radiographic image of the animal (Figure 2, *A* and *B*). The desired location of stent delivery was identified (Figure 2, *A*) and its inner diameter was measured at multiple sections in the radiographic image (Figure 2, *B*). We also desired to elastically preload the stent against the

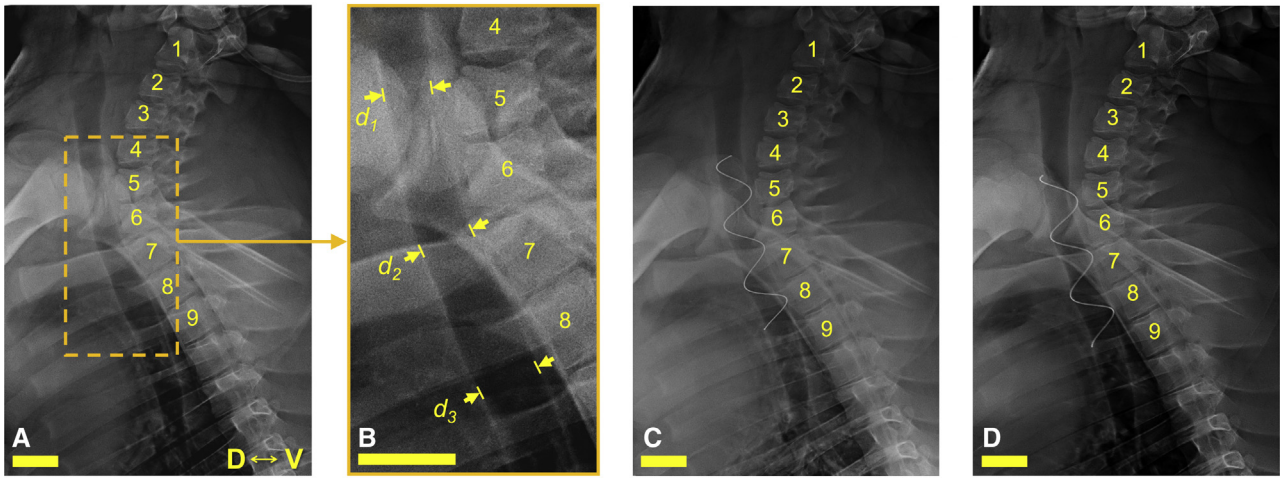

FIGURE 2. Radiographic images for tracheal size estimation and stent migration in swine trachea. Representative left lateral thoracic radiographic images for estimation of tracheal size (A and B) and monitoring stent migration (C and D). A, Radiographic image on day 0 before stent delivery with desired location of stent implantation in the trachea lying near the fourth and eighth vertebrae (*dotted orange rectangle*). B, Magnified view of desired stent delivery location. Estimation of trachea diameter at 3 sections (proximal to distal): $d_1 = 11.7$ mm, $d_2 = 12.7$ mm, and $d_3 = 14.5$ mm from radiographic images. Estimated average diameter = 13 mm. C, Radiographic image after delivery of trachea selected helical stent (outer diameter [OD] = 14.7 mm, number of coils [N_C] = 3) on day 0. D, The stent remained in its implanted position between fourth and eighth vertebrae on day 21. Scale bars: 20 mm. *D*, Dorsal; *V*, ventral.

tracheal wall to prevent migration along the trachea while also avoiding migration through the tracheal wall. Having measured the tracheal wall thickness to be >1 mm, stent diameter was selected to be 2 mm larger than the estimated average airway diameter. In this way, elastic preloading against the tracheal wall would go to 0 before penetration. Bronchoscopic examination of the airway was performed followed by stent placement. The animal was given a course of cephalexin (20 mg/kg) during recovery after stent implantation and banamine (1-2 mg/kg) to treat any inflammation as needed. Animal mentation was observed for 1 to 2 days for signs of any respiratory distress.

To monitor mucus clearance, polytetrafluoroethylene discs (1 mm diameter × 0.1 mm thickness) were dispensed uniformly in the stented region of the trachea, and distally to it, under brochoscopic guidance. Bronchoscopic examination was performed the following week to determine whether or not the discs had been cleared from the airway. In addition, radiographic images were taken immediately after stent placement and then weekly to assess stent position and migration in the trachea.

At the end of 4 weeks, the animals were put to death and the tracheas harvested (5 experimental and 2 control). The tracheas were divided into 2 lateral halves using dorsal to ventral cuts. The left half was used for tissue staining the right half was used for scanning electron microscopy (SEM).

Pathology

The tracheal tissue was fixed in 10% formaldehyde solution for 72 hours then washed in phosphate buffered saline and stored in 70% ethyl alcohol (EtOH). It was then cut longitudinally into rectangular sections (~7 mm × 50 mm), which spanned adjacent stented and unstented regions. Similar tissue sections were prepared from the control animals. The fixed tissue was then embedded in paraffin, and histologic slides were prepared by cutting 4 μm sections and staining with hematoxylin and eosin. The stained tissue on each slide was then demarcated into 7-mm subsections and classified as follows:

- Stented region with wire contact (SWC): Subsection includes tissue lying directly under wire of helical stent;
- Stented region with no wire contact (SNC): Subsection located within stented region, but not touching stent wire;
- Unstented (UT): Subsection outside of stented region; and
- Control (CL): Subsection from an unstented animal.

The slides were randomized and then reviewed by a pathologist (V.Y.J.) blinded to the animal group and subsection classification. The subsections on each slide were semiquantitatively assessed and graded for fibrosis, inflammation, granulation tissue, foreign body response, and tissue damage and extent (ie, involving surface epithelium, submucosa, and cartilage). Each variable was graded using a 4-tier scale: absent, low, medium, and high. Absent and low grades for each variable were considered within normal physiological spectrum.

SEM

Tissue samples were fixed in 4% methanol-free paraformaldehyde solution (Polysciences Inc, Warrington, Pa) for 24 hours. The tissue was then washed with phosphate buffered saline and dehydrated by submerging it in increasing concentration of EtOH solutions (25%, 50%, 75%, and 95% EtOH by volume) for 2 hours in each solution. Rectangular tissue sections, including regions in contact with the stent wire were cut and submerged in hexamethyldisilazane (Polysciences Inc) for 10 minutes. The tissue was then desiccated by vacuum drying. The desiccated tissue was mounted on a 12-mm diameter metal stub and sputter coated with 5 nm platinum/palladium 80/20 alloy (EMS 150T S Metal Sputter Coater; Quorum Technologies, Lewes, UK). SEM (EVO 55 Environmental SEM; ZEISS, Oberkochen, Germany) was performed across the stented region. Images were captured in sequence and stitched together extending across the width of the stent wire contact region. The width of the unciliated region in each tissue was measured and used for estimating the percentage of unciliated area per unit stented area.

RESULTS

In Vivo Experiment Outcomes and Recovery

Stents were successfully implanted and removed in the 5 animals without complications. Each animal was implanted with a single stent for the study duration. The animals did not exhibit any symptoms or respiratory distress associated with the stents. Results are summarized in Table 1.

Procedures

Stent delivery and removal (Video 1) were straightforward. Delivery time averaged 5.07 ± 2.69 minutes and removal time was 3.65 ± 3.70 minutes. Tracheal irritation was minor during stent delivery (Figure 3, *A*) and removal (Figure 3, *C*). In 3 animals, portions of the stent had become endothelialized and in 4 animals the proximal ball end, which needed to be grasped for removal, was endothelialized. In the latter cases, the forceps of the removal tool were successfully used to grasp the ball through the

TABLE 1. Stent selection and migration

Animal no.	Stent size: OD, N_C	In vivo procedure			Unciliated region width (μm)	Unciliated area per unit stented area (%)
		Stent migration	Stent deployment time (min)	Stent removal time (min)		
1	12.7 mm, 3	No	2.58	10.25	Coil #1: 812 Coil #3: 520	4.1
2	14.3 mm, 3	No	6.98	1.88	Coil #1: 869 Coil #2: 676 Coil #3: 652	4.4
3	14.3 mm, 3	No	2.32	2.65	Coil #1: 843 Coil #2: 595 Coil #3: 848	4.5
4	12.7 mm, 2	No	8.45	1.62	Coil #1: 1965	12.1
5	11.1 mm, 3	Yes	5.02	1.85	–	–

OD, Outer diameter; N_C, number of coils.

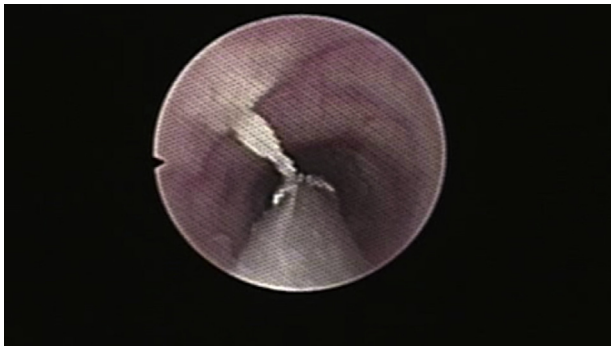

VIDEO 1. Stent removal. Video available at: https://www.jtcvs.org/article/S0022-5223(20)30572-9/fulltext.

endothelium. In all cases, the corkscrew motion of the tool for retracting the stent into the cannula was successful in minimizing tracheal abrasion during removal (Figure 3, *C*).

Stent Migration

Stent position in the weekly radiographic images was compared with the position measured immediately after placement (Figure 2, *C* and *D*). Stent position measured with respect to the vertebrae was noted to vary up to 4 mm. This variation is probably due to the difference in positioning of the animal during radiography. To the resolution of our measurements, the stents did not migrate in 4 out of 5 animals throughout the 3-week stenting period (Figure 2, *C* and *D*). Although stent migration was observed in 1 animal (#5) due to underestimation of tracheal diameter, the stent remained within the trachea and the animal did not exhibit any signs of respiratory distress throughout the 3-week stenting period.

Mucus Clearance

Mucus flow was maintained throughout the stenting period as well as after stent removal. The polytetrafluoroethylene discs dispensed over, and distal to, the stented section of tracheal wall each week were cleared and absent during the following week's bronchoscopic examination (Figure 3, *E-H*). Short-term mucus flow was also captured by recording video for 20 minutes after disc dispensing (Video 2). The observed flow pattern matches what was previously reported.[32] Flow on the lateral walls is directed at roughly 45° from the dorsal to ventral surfaces.

Pathology Review

Eleven longitudinal tracheal tissue sections were collected from the 4 experimental animals that did not experience stent migration (animals #1-4). Four tracheal tissue sections were also collected from 2 CL animals. The stained slides were divided into a total of 69 subsections of 7 mm width with 11, 25, 17, and 16 subsections categorized, respectively, as SWC, SNC, UT, and CL. Tissue was assessed with respect to inflammation, granulation tissue, fibrosis, and tissue damage, and extent. Representative microscopic images of all the tissue groups are presented

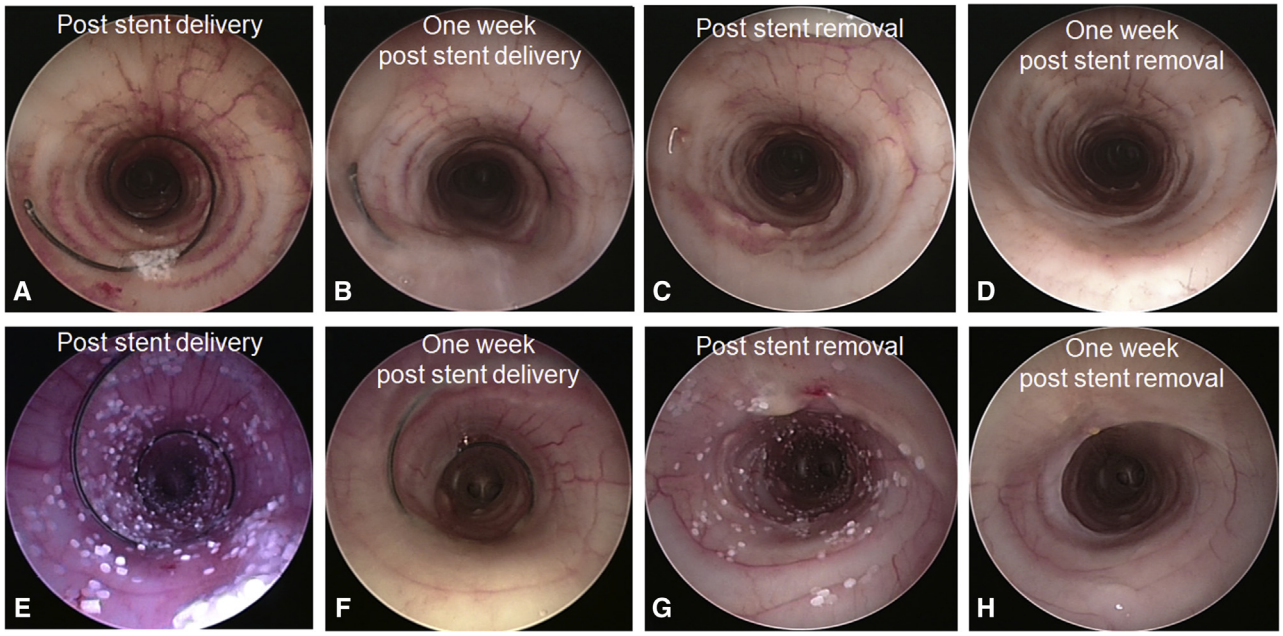

FIGURE 3. Endoscopic images of swine trachea. A, Immediately after stent placement. B, One week after stent delivery. C, Week 3 immediately after stent removal. D, Week 4; that is, 1 week after stent removal. E-H, Airway mucus flow assessment by clearance of dispensed polytetrafluoroethylene (PTFE) discs. E, PTFE discs distributed on trachea in stented region just after stent delivery. F, One week later PTFE discs have been cleared despite presence of stent. G, PTFE discs dispensed on trachea immediately after stent removal (week 3). H, Discs have been cleared 1 week later (week 4) indicating removal does not affect mucus clearance.

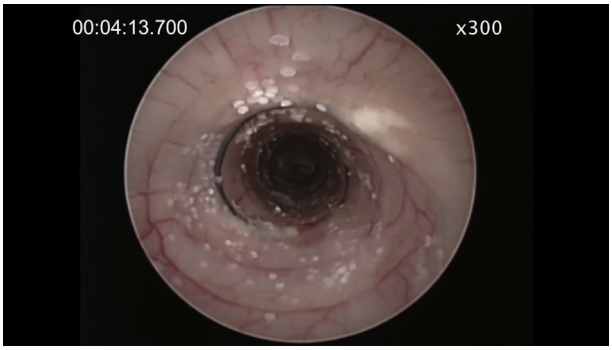

VIDEO 2. Mucus flow pattern. Video available at: https://www.jtcvs.org/article/S0022-5223(20)30572-9/fulltext.

in Figure 4. The results of the blinded review are summarized in Figure 5.

Figure 4, *A,* shows a representative slide of stented animal that included 2 coils of the stent (tissue subsection 2 and 4). The foreign body response components are significantly higher in these SWC subsections, which includes inflammation (Figure 4, *C*) and tissue fibrosis (Figure 4, *E*). The adjoining SNC tissue subsections on the other hand show low levels of foreign body response comparable to those in UT regions (Figure 4, *F*) and even control animals (Figure 4, *G*). Figure 5 summarizes the histological evaluation of tissues collected from all the experimental and control animals.

With respect to inflammation, granulation tissue formation, and fibrosis, these secondary effects of the stent were highly localized within the subsections in which the stent wire was in direct contact with the tissue. Those sections without wire contact (SNC and UT) were comparable to those from the control animals (CL subsections). Only for tissue damage did the effect of the stent extend into the SNC subsections, and this damage was graded as mild. Mild inflammation (composed of mostly lymphocytes) was observed in SNC and UT subsections, but this was judged to be within the spectrum of normal physiologic response.

The SWC subsections showed macrophage levels to be high in 18% and medium in 36% of the tissue subsections (Figure 5, *C*) indicative of foreign body clean up and injury repair. Components of acute inflammation (eosinophils [Figure 5, *A*] and neutrophils [Figure 5, *B*]) were low or absent in >80% of SWC subsections as expected because the stent had been removed 1 week before tissue harvest. There was no foreign body giant cell reaction in any of the tissue subsections, indicating absence of granulomatous inflammation associated with infection, autoimmune, toxic, allergic, drug, and neoplastic conditions. Formation of granulation tissue (Figure 5, *G*) was observed to be high in 9% and medium in 45% of SWC subsections. About 40% of SWC tissue subsections exhibited medium level of fibrosis (Figure 5, *H*) present in the subepithelial layer. There was evidence of tissue damage in response to direct contact with the stent in SWC subsections. About 25% of SWC tissue subsections had severe to moderate damage in the epithelial layer (Figure 5, *I* and *J*).

Distribution of Cilia

SEM imaging was used to determine over what region the stent affected the distribution of cilia on the epithelium in the 4 animals in which the stent did not migrate. Matching the results of the mucus clearance testing (Video 2), it was observed that the cilia were present everywhere in the stented regions except in the neighborhood where the stent wire contacted tissue (Figure 6). The width of the unciliated region averaged over 9 tracheal tissue samples was 874 ± 402 μm, which is less than twice the wire diameter of 510 μm. This result also tends to confirm our radiograph observations that the stents did not migrate in these 4 animals. The unciliated area per unit stented area in the 4 animals ranged from 4.1% to 12.1% (Table 1). In ideal conditions, only the area below the stent wire (width = wire diameter) would be unciliated and the area effected would be 3% to 3.3% of the stented area.

DISCUSSION

Our experiments confirm the benefits of a helical stent design (Figure 7). When properly sized, the screw-like shape of the stent resists migration as evidenced by our radiography and SEM studies. Estimation of tracheal diameter for stent selection is important because an undersized stent can migrate along the trachea, whereas an oversized stent could migrate through the tracheal wall. With tracheal wall thicknesses in our animal model in the range of 1.2 to 2.2 mm, we selected stent diameters 2 mm larger than the inner tracheal diameter as measured by radiograph. This value was sufficient to prevent migration while also avoiding tracheal penetration.

The foreign body response and tissue damage is localized to the region of stent wire contact (~4%-12%) leaving most (~88%-96%) of the stented region (which lies between the wire loops) unaffected. This enables mucus to flow through the stented region with the wire perhaps acting only as a speedbump, but not stopping the flow as in the case of silicone or covered metallic stents where foreign body contact is close to 100%. Mucus clearance was maintained throughout the stenting period as well as after removal and the animals did not require suctioning or any other form of assistance.

An additional benefit of the helical design is the ability to remove the stent, even when endothelialized, by using an unscrewing motion matching the pitch of the helix. This substantially reduces the trauma compared with the removal of a standard mesh stent. The pathologic features and SEM images both confirm that tissue damage, arising both from having the stent in place and from removing it, are localized to the contact regions with the stent wire.

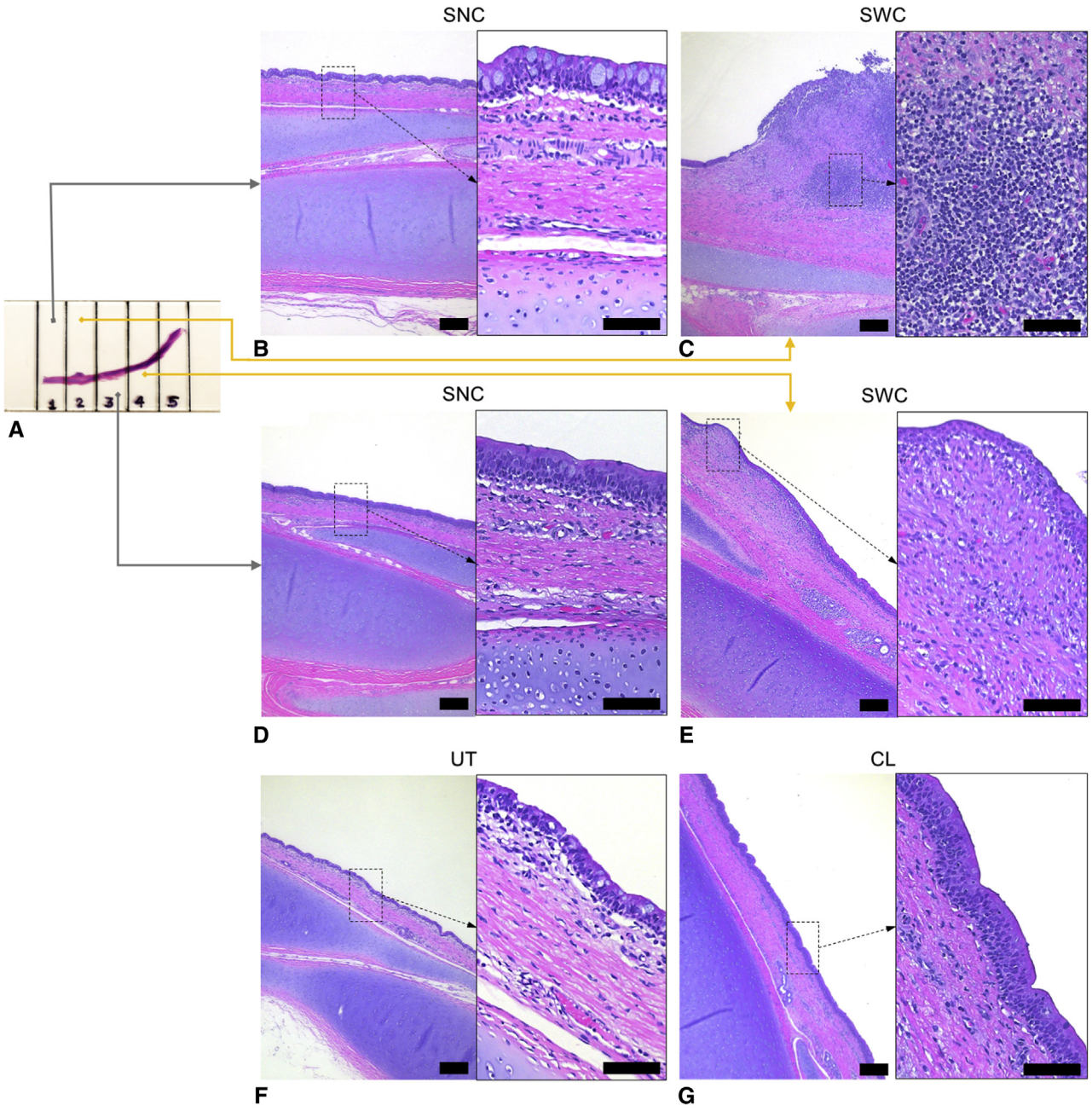

FIGURE 4. Hematoxylin and eosin stained lateral tracheal sections from a stented and a control (*CL*) animal. A, Tracheal sections are divided into 7 mm wide subsections. Stent wire contact regions (*SWC*) are positioned in center of subsections 2 and 4. Regions 1, 3, and 5 are in-between or adjacent to the stent wire and are thus classified as stented with no wire contact (*SNC*). B-E, Images at magnification 5× (*left image*) scale bar: 200 μm and 20× (*right image*) scale bar: 100 μm in SWC and stented with no wire contact (SNC) subsections. C, Inflammation and granulation levels were high in stented subsection 2. E, Inflammation and granulation levels were medium in stented subsection 4. The high level of inflammation in C (*right image*) shows densely confluent cellular areas primarily composed of numerous lymphocytes and macrophages. The medium level of inflammation in E (*right image*) shows infiltration of lymphocytes and macrophages, occasionally clustered in groups. B and D, SNC subsections 1, 3, and 5 (not shown) had low inflammation and no granulation or fibrosis, comparable to an unstented (*UT*) tissue sample from the same animal (F) and from a control animal (G).

Pathologic assessment of response to placement of the stent showed that inflammation, granulation tissue formation, and fibrosis were confined to the area of the trachea that were in direct contact with the stent (SWC). Because the fibrosis was subepithelial, it had no effect on the ciliated mucosal function. Furthermore, the SWC sections were the primary areas showing tissue damage secondary to the foreign body, evidenced by increased moderate-to-

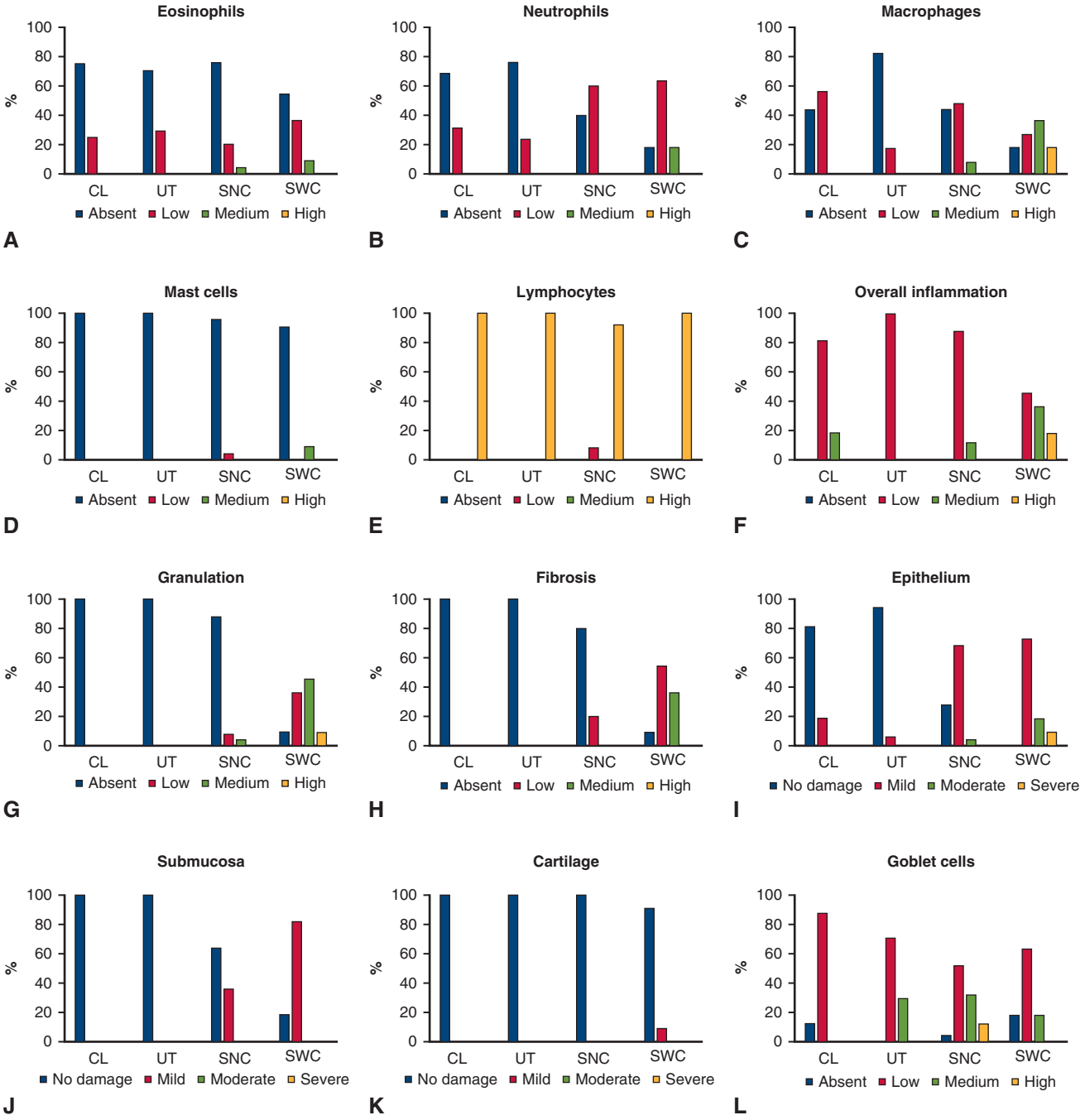

FIGURE 5. Normalized comparison of stented and control tissue in terms of inflammation, granulation, fibrosis, and tissue damage. Tissue subsections (n = 69) were semiquantitatively assessed and graded by pathologist blinded to tissue classification (control [*CL*], unstented [*UT*], stented region with no wire contact [*SNC*], or stented region with wire contact [*SWC*]) on the presence of eosinophils (A), neutrophils (B), macrophages (C), mast cells (D), lymphocytes (E), overall inflammation (F), granulation tissue (G), fibrosis (H), and tissue damage in the epithelium (I), submucosa (J), and cartilage (K). A 4-tier scale was used for grading: absent/no damage (*blue bars*), low/mild (*red bars*), medium/moderate (*green bars*) or high/severe (*yellow bars*). Each bar represents the percentage of tissue subsections in each grade normalized to the total number of tissue subsections in the respective tissue group (n = 16, 17, 25, and 11 for CL, UT, SNC, and SWC, respectively).

severe tissue damage. This damage was primarily observed in the superficial epithelial layers, and only mild tissue damage was seen in adjacent SNC subsections. These findings, in conjunction with observations of only localized loss of cilia in the areas of direct stent contact and maintained mucus flow, indicate that tissue reaction

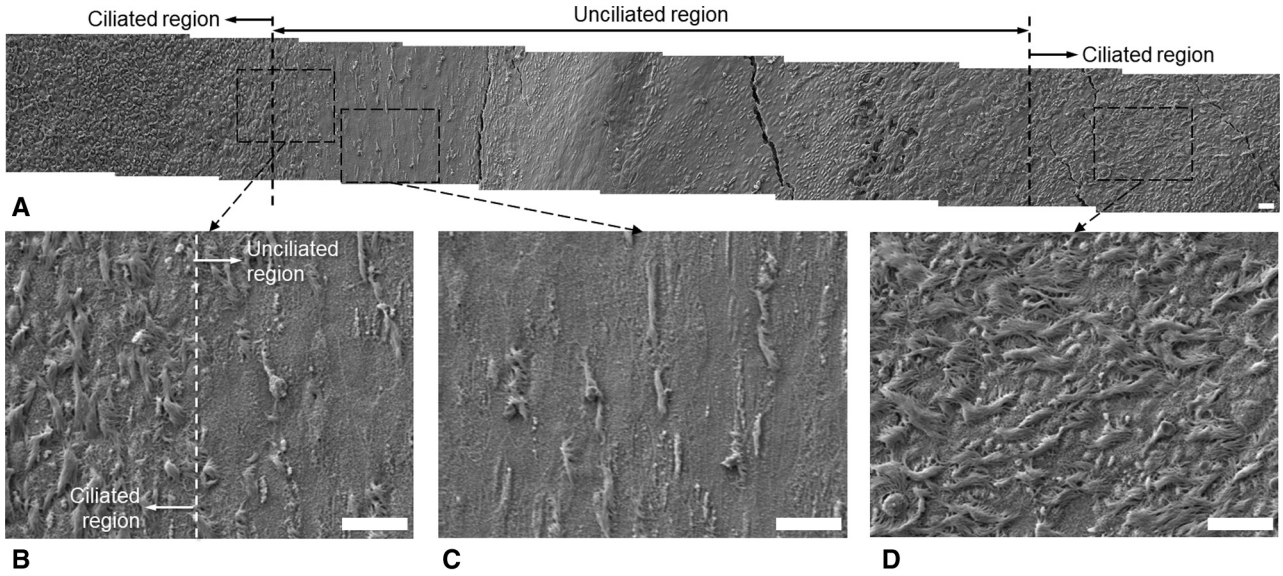

FIGURE 6. Scanning electron microscope images of ciliated regions. A, Composite image crossing stent wire contact region. Wire was oriented vertically with contact roughly centered in the unciliated region (*between black dotted lines*). B, Magnified view of border between with ciliated (*left of dotted line*) and unciliated (*right of dotted line*) epithelium. C, Magnified view of unciliated region. D, Magnified view of ciliated region. Scale bars: 20 μm.

and tissue damage are localized to areas of direct contact with the stent, and neighboring tracheal regions are only minimally affected.

While the SWC sections showed increased inflammation, granulation tissue, and fibrosis, these changes were largely absent in SNC sections. The primary component of the inflammatory response was lymphocytes and macrophages; foreign body giant cell response was not a feature. The findings in SWC and SNC 1-week poststent removal are features of tissue repair and damage resolution (granulation tissue) with no to low level of active damage (eg, low acute inflammation components in Figure 5, *A* and *B*). Furthermore, there are areas of intact mucosa overlying the SWC and SNC areas indicating tissue regeneration. Overall, these indicate that the tissue damage is not permanent and overall function is restored.

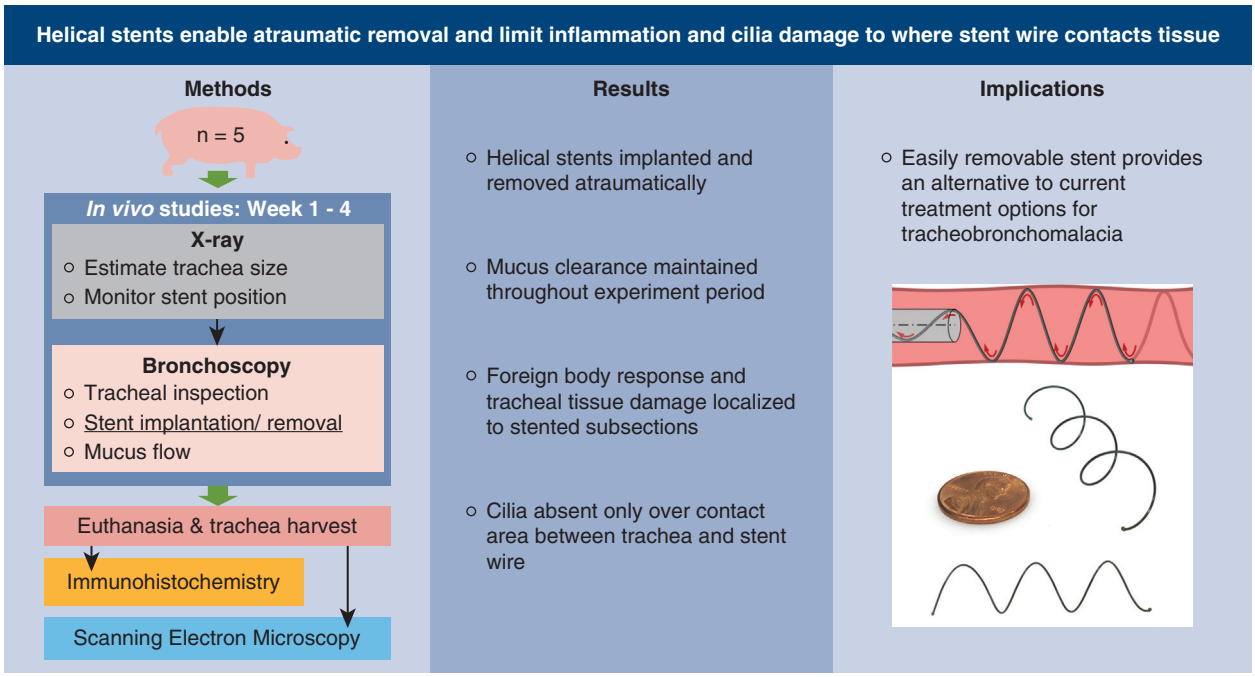

FIGURE 7. Helical stents enable atraumatic removal and limit inflammation and cilia damage to where the stent wire contacts tissue.

Limitations

Our study was performed in healthy swine because these were proof-of-concept experiments intended to assess the short-term effects of the stent on healthy tissue. Malacic airway models; that is, the fracture[31] or surgical removal[33] of tracheal cartilage, create significant trauma that can be difficult to distinguish from stent-induced effects. Nevertheless, future experiments should involve a malacic animal model to assess efficacy in maintaining airway patency.

The 3-week implantation period of our study was selected as sufficient to assess in vivo stent delivery, removal, and migration as well as mucus flow and short-term inflammatory response. Because positive pressure ventilation periods for tracheobronchomalacia can be up to 9 months, longer-term testing is needed. Such tests will enable assessment of long-term foreign body response, including the formation of granulation tissue, the extent of endothelialization, and the reliability of atraumatic removal after extended implantation.

CONCLUSIONS

This study demonstrates how a helical self-expanding stent can overcome the challenges of existing stent designs. Its screw-like geometry can provide radial support to the airway while resisting migration, minimally impeding mucus flow, and enabling easy removal using an unscrewing motion. Further studies are needed to assess the long-term performance of the stent.

Conflict of Interest Statement

Drs Dupont, Kaza, and Ha are inventors on a US patent application held by Boston Children's Hospital that covers the stent technology. Dr Jo discloses her spouse's employment at Merck and Co. All other authors have nothing to disclose with regard to commercial support.

References

1. Holinger LD. Etiology of stridor in the neonate, infant and child. *Ann Otol Rhinol Laryngol*. 1980;89:397-400.
2. Boogaard R, Huijsmans SH, Pijnenburg MWH, Tiddens HAWM, De Jongste JC, Merkus PJFM. Tracheomalacia and bronchomalacia in children: incidence and patient characteristics. *Chest*. 2005;128:3391-7.
3. Berrocal T, Madrid C, Novo S, Gutiérrez J, Arjonilla A, Gómez-León N. Congenital anomalies of the tracheobronchial tree, lung, and mediastinum: embryology, radiology, and pathology. *RadioGraphics*. 2004;24:e17.
4. Lee EY, Restrepo R, Dillman JR, Ridge CA, Hammer MR, Boiselle PM. Imaging evaluation of pediatric trachea and bronchi: systematic review and updates. *Semin Roentgenol*. 2012;47:182-96.
5. Weigle CGM. Treatment of an infant with tracheobronchomalacia at home with a lightweight, high-humidity, continuous positive airway pressure system. *Crit Care Med*. 1990;18:892-4.
6. Pizer BL, Freeland AP, Wilkinson AR. Prolonged positive airway pressure for severe neonatal tracheobronchomalacia. *Arch Dis Child*. 1986;61:908-9.
7. Panitch HB, Allen JL, Alpert BE, Schidlow DV. Effects of CPAP on lung mechanics in infants with acquired tracheobronchomalacia. *Am J Respir Crit Care Med*. 1994;150(5 Pt 1):1341-6.
8. Chastre J, Fagon J-YY. *Ventilator-Associated Pneumonia*, 165. New York, NY: American Thoracic Society; 2002:867-903.
9. Cooper JD, Pearson FG, Patterson GA, Todd TR, Ginsberg M, Goldberg M, et al. Use of silicone stents in the management of airway problems. *Ann Thorac Surg*. 1989;47:371-8.
10. Dumon J-F. A dedicated tracheobronchial stent. *Chest*. 1990;97:328-32.
11. Beamis JF, Mathur PN, Beamis JF, Becker HD, Cavaliere S, Colt H, et al. ERS/ATS statement on interventional pulmonology. *Eur Respir J*. 2002;19:356-73.
12. AARC. AARC Clinical Practice Guidelines. Endotracheal suctioning of mechanically ventilated patients with artificial airways 2010. *Respir Care*. 2010;55:758-64.
13. Clifton-Koeppel R. Endotracheal tube suctioning in the newborn: a review of the literature. *Newborn Infant Nurs Rev*. 2006;6:94-9.
14. Kumar P, Roy A, Penny DJ, Ladas G, Goldstraw P. Airway obstruction and ventilator dependency in young children with congenital cardiac defects: a role for self-expanding metal stents. *Intensive Care Med*. 2002;28:190-5.
15. Public health notification. Complications from metallic tracheal stents in patients with benign airway disorders. 2005. Available at: http://www.fda.gov/MedicalDevices/Safety/AlertsandNotices/PublicHealthNotifications/ucm062115.htm. Accessed October 15, 2015.
16. Lischke R, Pozniak J, Vondrys D, Elliott MJ. Novel biodegradable stents in the treatment of bronchial stenosis after lung transplantation. *Eur J Cardiothorac Surg*. 2011;40:619-24.
17. Dutau H, Musani AI, Laroumagne S, Darwiche K, Freitag L, Astoul P. Biodegradable airway stents—bench to bedside: a comprehensive review. *Respiration*. 2015;90:512-21.
18. Antón-Pacheco JL, Luna C, García E, López M, Morante R, Tordable C, et al. Initial experience with a new biodegradable airway stent in children: is this the stent we were waiting for? *Pediatr Pulmonol*. 2016;51:607-12.
19. Chao YK, Liu KS, Wang YC, Huang YL, Liu SJ. Biodegradable cisplatin-eluting tracheal stent for malignant airway obstruction: in vivo and in vitro studies. *Chest*. 2013;144:193-9.
20. Novotny L, Crha M, Rauser P, Hep A, Misik J, Necas A, et al. Novel biodegradable polydioxanone stents in a rabbit airway model. *J Thorac Cardiovasc Surg*. 2012;143:437-44.
21. Saito Y, Minami K, Kobayashi M, Nakao Y, Omiya H, Imamura H, et al. New tubular bioabsorbable knitted airway stent: biocompatibility and mechanical strength. *J Thorac Cardiovasc Surg*. 2002;123:161-7.
22. Morrison RJ, Hollister SJ, Niedner MF, Mahani MG, Park AH, Mehta DK, et al. Mitigation of tracheobronchomalacia with 3D-printed personalized medical devices in pediatric patients. *Sci Transl Med*. 2015;7:285ra64.
23. Zopf DA, Hollister SJ, Nelson ME, Ohye RG, Green GE. Bioresorbable airway splint created with a three-dimensional printer. *N Engl J Med*. 2013;368:2043-5.
24. Vondrys D, Elliott MJ, McLaren CA, Noctor C, Roebuck DJ. First experience with biodegradable airway stents in children. *Ann Thorac Surg*. 2011;92:1870-4.
25. Sztanó B, Kiss G, Márai K, Rácz G, Szegesdi I, Rácz K, et al. Biodegradable airway stents in infants—potential life-threatening pitfalls. *Int J Pediatr Otorhinolaryngol*. 2016;91:86-9.
26. Sztano B, Rovo L. Response to the letter to the Editor "Biodegradable airway stents in infants—potential life-threating pitfalls". *Int J Pediatr Otorhinolaryngol*. 2017;98:175-6.
27. Vondrys D, Anton-Pacheco Sanchez J. Letter to the Editor regarding "Biodegradable airway stents in infants—potential life-threatening pitfalls". *Int J Pediatr Otorhinolaryngol*. 2017;98:174.
28. Ha J, Mondal A, Zhao Z, Kaza AK, Dupont P. Pediatric airway stent designed to facilitate mucus transport and atraumatic removal. *IEEE Trans Biomed Eng*. 2020;67:177-84.
29. Korpela A, Aarnio P, Sariola H, Törmälä P, Harjula A. Bioabsorbable self-reinforced poly-L-lactide, metallic, and silicone stents in the management of experimental tracheal stenosis. *Chest*. 1999;115:490-5.
30. Schopf LF, Fraga JC, Porto R, Santos LA, Marques DR, Sanchez PR, et al. Experimental use of new absorbable tracheal stent. *J Pediatr Surg*. 2018;53:1305-9.
31. Tsugawa C, Nishijima E, Muraji T, Yoshimura M, Tsubota N, Asano H. A shape memory airway stent for tracheobronchomalacia in children: an experimental and clinical study. *J Pediatr Surg*. 1997;32:50-3.
32. Hilding AC. Ciliary streaming in the lower respiratory tract. *Am J Physiol*. 1957;191:404-10.
33. Tsukada H, O'Donnell CR, Garland R, Herth F, DeCamp M, Ernst A. A novel animal model for hyperdynamic airway collapse. *Chest*. 2010;138:1322-6.

Key Words: tracheobronchomalacia, airway stent, preclinical validation